MICROSTRUCTURE, DEFECTS AND FATIGUE BEHAVIOR OF CAST AlSi7Mg ALLOY

Stanislava Fintová[1)], Radomila Konečná[1)], Gianni Nicoletto[2)]*
[1)] University of Žilina, Faculty of Mechanical Engineering, Žilina, Slovakia
[2)] University of Parma, Faculty of Engineering, Parma, Italy

Received: 07.10.2012
Accepted: 20.05.2013

[*]Corresponding author: e-mail: radomila.konecna@fstroj.uniza.sk, Tel.: +421 415132604, Department of Materials Engineering, Faculty of Mechanical Engineering, University of Žilina, Univerzitná 1, 010 26 Žilina, Slovakia,

Abstract
The cast AlSi7Mg alloy prepared using different modifier was studied. The main factor influencing fatigue properties were the casting defects. Using metallography and statistical approach, Larger Extreme Value Distribution (LEVD) theory, the structure and the porosity were evaluated. According to the largest defects sizes prediction fatigue tests were performed. Fatigue cracks were initiated on the casting defects present on the specimen free surface or just below the surface identified using SEM. Specimens fatigue life was influenced by the size of the defect in the initiation place and the number of initiation places. The specimens fatigue behaviour corresponded with the assumptions according to the LEVD.

Keywords: aluminium alloy, casting, defects, fatigue

1 Introduction

Cast aluminum alloys are increasingly used in the automotive industry due to their excellent castability, corrosion resistance, and especially their high strength-to-weight ratio. Their application for cast components subjected to dynamic loading has motivated considerable interest on the fatigue behavior of cast Al-Si alloys. Besides the microstructural characteristics, fatigue strength of cast aluminum components heavily depends on the casting defects formed during solidification because they favor fatigue crack initiation due to high local stress concentration [1].

The fatigue properties of Al-Si alloys are influenced besides the porosity also by the structural features like the dendrites fineness, intermetallic phases and the materials heat treatment [2]. In the case of the presence of the casting defects the influence of the structural features play just a minor role [3, 4, 5].

The defects often result in poor mechanical properties including limited strength and ductility, variable fracture toughness, irregular crack initiation and crack propagation characteristics, potentially accompanied by a lack of pressure tightness [6]. The effect of porosity on fatigue life has been summarized as follows: pores reduce the time for crack initiation by creating a high stress concentration in the material adjacent to the pores; because of this, most of the fatigue life is spent in crack growth [7].

There exists a critical defect size, [3], (in Sr modified cast A356 alloy, the critical defect size is in the range of 25-50 μm) for fatigue crack initiation, below which the fatigue crack initiates from other intrinsic initiators such as eutectic particles and slip bands.

DOI 10.12776/ams.v19i3.164 p-ISSN 1335-1532
e-ISSN 1338-1156

In this contribution the influence of the porosity on the fatigue behavior of cast AlSi7Mg alloys is studied. The used specimens were prepared using different modifiers and casting process. From the obtained bars the specimens for the metallographic evaluation, and also the porosity evaluation using the metallographic methods, and the specimens for the fatigue tests were prepared. After the porosity evaluation according to the Largest Extreme Value Distribution (LEVD) theory [8] the fatigue tests were planed and performed. The fatigue fracture surfaces of the specimens broken during the fatigue tests were examined using SEM and the fatigue crack initiation places were identified. At the end all the obtained results were confronted and the relations between them were found.

2 Experimental material(s) and methods

As the experiment material the cast AlSi7Mg alloy in this study was used. The studied specimens were mould casted in the shape of bars. From each bar, the metallographic specimens and the smooth 6 diameter specimens for the rotating bending fatigue test were prepared. The casted specimens were divided into 6 batches, according to the casting process and used modifier, see **Table 1**. For each batch five bars were cast.

Table 1 Specification of individual specimen batches

Batch	Casting process specification
2	cast after the modification by pure Na
3	cast after the subsiding of the modification effect of Na
4	cast after the modification by sodium salts and degassing by N during 10 min
5	cast after the subsiding of the modification effect of Na salts and degassing
6	cast after the modification by Sr
7	cast after the modification by Sr and gassing by the Begaser tablets

After the casting, the bars were treated by heat treatment T6 consisting in solution annealing and artificial aging.

Each specimen was examined by metallographic methods. The microstructure of the specimen was defined by the SDAS (Secondary Dendrite Arm Spacing) factor and also the casting defects using the image analysis program NIS Elements 3.0 were evaluated. The casting defect sizes present in the microstructure were evaluated using Murakami's approach based on statistical method Largest Extreme Value Distribution (LEVD) theory.

For the estimation of the actual defect size different approaches for the defects size characterization were used. Typical equivalent size definitions found in the literature are: $area^{1/2}$, $4(area)^{1/2}/\pi$, Feret diameter [1, 8, 9, 10]. In this contribution, the most used [8, 11] the $area^{1/2}$ and the maximum Ferret diameter as the defects size describing values were used.

The Murakami's approach is based on the evaluation of the largest defect size on the field of view. In this method a number, n, of separated regions (control areas), each with the same area S_0 of the selected image magnification, are chosen on the polished surface of metallographic sections, and the equivalent size, $area^{1/2}$, of the largest pore within each region is recorded. The result is a set of n observations of maximum sizes $area^{1/2}$ and the Gumbel distribution [8] is fitted to these data. Under the Gumbel distribution the points are expected to lie close to the line. The fitted distribution is then used to estimate the size of the largest defect size in a given region S larger than the control area S_0, through the return period $T = S/S_0$, or to compare largest defects from control areas of different sizes.

DOI 10.12776/ams.v19i3.164 p-ISSN 1335-1532
e-ISSN 1338-1156

Because of the influence of the casting defects on the fatigue crack initiation and growth, this prediction can be used in planning the fatigue test conditions of the specimens. The rotating bending fatigue tests, with the 50 Hz frequency and R = -1, were performed. The stress amplitudes of the tests were in the range from 80 to 20 MPa.
After the specimens failure the fatigue surfaces were examined using the Scanning Electron Microscope (SEM) to identify and count the fatigue crack initiation places. All the obtained results were at the end compared and their dependence and mutual influences were discussed.

3 Results and discussion

3.1 Microstructure and defects

The microstructure of the cast AlSi7Mg alloy consists of the α-phase dendrites – light grey (solid solution of Si in Al) and eutectic (α-phase and dark grey Si particles) situated in interdendritic spaces, **Fig. 1a**. The SDAS factor values which describe the secondary dendrite arm spacing are in the range 20-25 μm and similar for each batch.

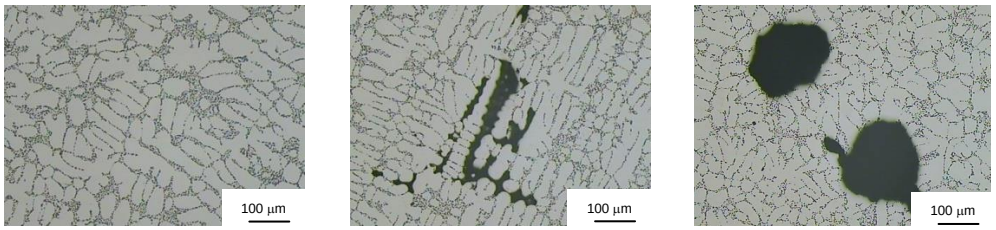

a) microstructure b) microshrinkage pores c) gas pores

Fig. 1 Typical microstructure and casting defects present in AlSi7Mg castings, etched by 0.5% HF

In the specimens microstructure almost in all the cases the large amount of casting defects was observed. In all the cases, except the batch 7, only the microshrinkage pores were present. In the specimens from the batch 7, because of the gassing of the liquid metal before the casting, the large gas pores and just a small amount of microshrinkage pores with the size smaller compare to the gas pores were present. The microshrinkage pores created during the solidification process are complicated in the shape and are located in the interdendritic location near the dendrites, **Fig. 1b**. The microshrinkage pores are observed on the metallographic cross section in clusters consisting from larger and smaller microshrinkage pores which can be just cut branches of one bigger shrinkage pore. The gas pores are present in the castings because of the gas saturation of the melted metal during the casting process. The gas pores are rounded in the shape and they are almost always present in the casting individually, **Fig. 1c**. In general, the gas pores should be less dangerous, in term of the fatigue crack initiation, compare to the microshrinkages [12, 13].
The arrangement of the casting defects was evaluated on the specimen's macrographs shown on **Fig. 2**. In the case of the specimens from the batches 2 and 6 the microshrinkage pores were present in the entire specimen surface, also on the specimens' free surfaces and close to them, **Fig. 2a**. In the case of the specimens from the batches 3, 4 and 5 only the small amount of defects was observed, **Fig. 2b**. The gas pores present in the specimens from the batch 7 were like in the case of the defects in the specimens from the batches 2 and 6 arranged in all the specimens' cross section and also in the fatigue crack critical localities – on the specimens' free surfaces and close to the specimens' free surfaces, **Fig. 2c**.

DOI 10.12776/ams.v19i3.164 p-ISSN 1335-1532
e-ISSN 1338-1156

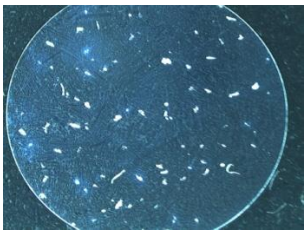
a) microshrinkage pores, batches 2 and 6

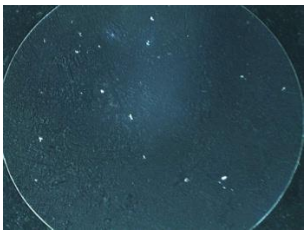
b) microshrinkage pores, batches 3, 4 and 5

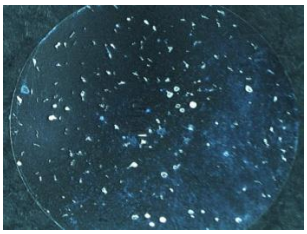
c) gas pores, batch 7

Fig. 2 Macrographs of metallographic specimens, stereomicroscope, mag. 6.3 x

In almost all of the evaluated specimens the presence of the intermetallic phases, which are in general considered as undesirable, were observed, **Fig. 3**.

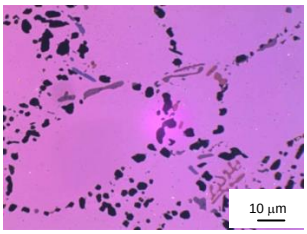

a) $FeSiAl_5$ needles, Al(Fe, Mg)Si massive and Chinese script shape particles

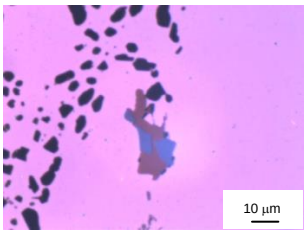

b) Al(Fe, Mg)Si massive particles

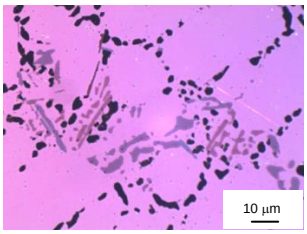

c) $FeSiAl_5$ needles, Al(Fe, Mg)Si massive particles

Fig. 3 Intermetallic phases, etched by Ammonium Molybdate, polarized light

Even though the intermetallic phases can have a negative influence on the material properties and can be the initiating places for the fatigue cracks. In this case, the size and the amount of the present intermetallic phases was not sufficient to act as the fatigue crack initiators and so as the main factor for the fatigue properties decreasing the casting defects were identified. The size and the amount of the present defects were much larger compare to the present intermetallic phases.

3.2 The largest defect size prediction

The porosity of the specimens was evaluated on the light optical microscope Neophot 32 using the image analysis program NIS Elements 3.0. The used magnification was 50 x and the inspected area size was $S_0 = 1.62$ mm^2. The largest defects were described by two different sizes the area$^{1/2}$ and the max. Ferret diameter sizes. The measured values are plotted to the LEVD graphs of **Fig. 4**.

Scatter of the fatigue data is typical of cast Al-Si alloys. When the number of specimens is limited, the plot describing the largest pore sizes for the individual batches of **Fig. 4** can be used to in planning the fatigue experiments. When the slope value is high the fatigue behavior of the material should be less scattered, when the slope value is low the fatigue scatter is large. For predicting the expected largest pore sizes in specimens, the data of **Fig. 4** were extrapolated to the area S = 10 mm^2 (the most stressed area of the specimens for the rotating bending fatigue tests) which is typical for small castings and the results are given in **Table 2**. In all the cases the predicted largest defect sizes are larger than the critical defect size for the preferential initiation of the fatigue crack (20 - 50 µm, [3]).

DOI 10.12776/ams.v19i3.164 p-ISSN 1335-1532
e-ISSN 1338-1156

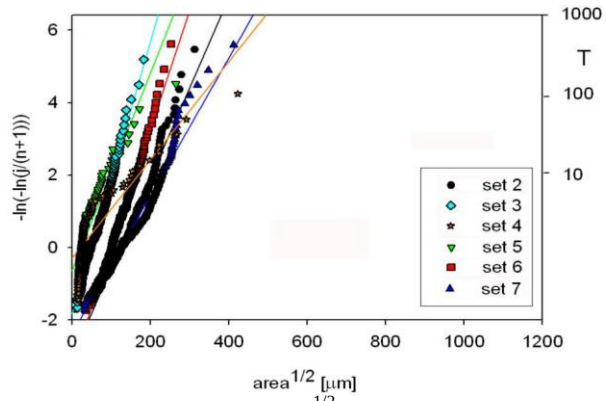

a) LEVD porosity plot - area$^{1/2}$

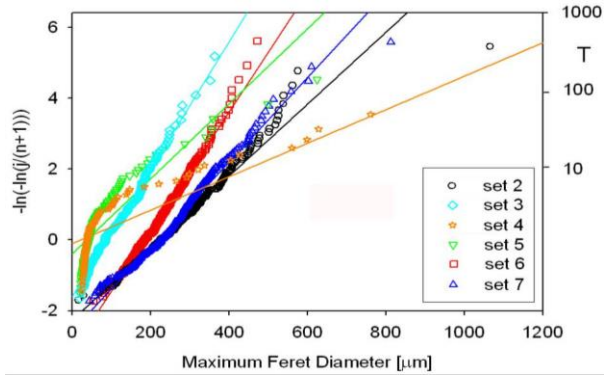

b) LEVD porosity plot – max. Ferret diameter

Fig. 4 LEVD porosity plots

In this case, the fatigue cracks will be initiated on the casting defects and the structural features will have just minor effect on the fatigue crack initiation.
Smaller defects sizes (i.e. area$^{1/2}$) for the area S = 10 mm^2 were predicted for the specimens from the batches 4 (cast after the modification sodium salts and degassing by N during 10 min.) and 5 (cast after the subsiding of the modification effect of Na salts and degassing). Larger defects sizes were predicted for the specimens from the batches 3 (cast after the subsiding of the modification effect of Na) and 6 (cast after the modification by Sr). The largest defects sizes area$^{1/2}$ for the area S = 10 mm^2 were predicted for the specimens from the batches 2 (cast after the modification by pure Na) and 7 (cast after the modification by Sr and gassing by the Begaser tablets). In the case of the defects description by the max. Ferret diameter values the trend predicted results is the same as in the case of the area$^{1/2}$ predictions (**Table 2**).

3.3 Fatigue tests

The fatigue behavior was expected to correlate with the defect size of the predictions of **Table 2**. Therefore, the fatigue behavior of the specimens from the batches 4 and 5 was expected to be the best, followed by the batches 3 and 6 and the worst being the batches 2 and 7. Stress amplitudes applied to the specimens were relatively high (60 - 80 MPa) for batches with the small predicted defects sizes and low (40 – 20 MPa) for batches with expected large defects. From the fatigue

DOI 10.12776/ams.v19i3.164 p-ISSN 1335-1532
e-ISSN 1338-1156

tests results shown in the **Table 3** it is possible to compare the influence of the used modifier (**Table 1**) on the fatigue behavior of tested batches. In the case of the specimens tested on the same stress level, it is possible to compare also the influence of the predicted largest defect size (**Table 2**) on the reached number of cycles to failure (N_f).

Table 2 Predicted largest defect size for the area S = 10 mm^2

Specimen	Predicted largest defect size for the area S = 10 mm^2		Specimen	Predicted largest defect size for the area S = 10 mm^2	
	area$^{1/2}$[μm]	max. Ferret diameter [μm]		area$^{1/2}$[μm]	max. Ferret diameter [μm]
2E	153	315	3B	88	171
2C	184	335	3E	95	186
2A	196	414	3D	102	199
2B	210	498	3C	106	201
2D	225	419	3A	100	202
4C	43	77	5D	43	91
4D	43	102	5C	56	113
4A	56	98	5A	65	133
4E	111	263	5B	74	159
4B	246	657	5E	165	403
6E	123	247	7E	163	292
6D	132	256	7B	187	433
6B	145	272	7C	242	343
6C	160	315	7D	230	352
6A	193	347	7A	248	357

The fatigue tests results show that the best fatigue properties are reached with the specimens of batch 3 (i.e. cast after the subsiding effect of modification by pure Na, **Table 1**). At comparable stress amplitudes, the fatigue lives for batch 5 (cast after the subsiding of the modification effect of sodium salts and degassing) are longer than for batch 4 (cast after the modification by sodium salts and degassing by N during 10 min.). Both batches were prepared using Na as modifier and after degassing and the fatigue behavior follows the expectation based on the largest pore sizes, **Table 2**.

The influence of the type of modifier did not influence significantly the fatigue behavior: batch 2 (cast after the modification by pure Na) and batch 7 (and cast after the modification by Sr and gassing by the Begaser tablets) have comparable results. This observation agrees with the comparable predicted largest defects sizes according to the LEVD theory, **Table 2**. Even the shape of defect, i.e. ramified (microshrinkage) or round (pore), apparently does not influence markedly the fatigue crack initiation.

Finally, the fatigue behavior of the specimens cast after the modification by Sr (batch 6) is highly scattered and the pore size predictions were not successful in guiding the fatigue test planning. There is probably some additional factor besides porosity that affects the fatigue behavior.

DOI 10.12776/ams.v19i3.164 p-ISSN 1335-1532
e-ISSN 1338-1156

Table 3 Fatigue test results

Specimen	S_a [MPa]	N_f [cycles to failure]	Specimen	S_a [MPa]	N_f [cycles to failure]
2E	80	39	3B	88	2 081 850
2C	50	7 549	3E	70	861 858
2A	35	176 481	3A	65	74
2B	30	1 751 395	3C	60	844 393
2D	25	40 179	3D	60	5 271
4C	80	41	5E	165	36
4D	50	104 655	5B	74	962 505
4E	40	97	5A	65	439 338
4A	35	12 463 211	5C	56	99
4B	30	2 360 844	5D	43	670 789
6E	80	60	7E	80	49
6D	50	41	7B	50	2 956
6B	35	1 259	7C	35	380 467
6C	25	487	7D	30	54 957
6A	20	40	7A	30	45 187

3.4 Fractographic analysis of the fatigue fracture surfaces

After the fatigue tests due to the initiation places identification the fracture surfaces of the broken specimens on the SEM VEGA Tescan were examined.

Because of the casting process the defects on the fracture surfaces were found. The defects were present in the entire broken surface of the specimens and also on the specimens' free surface. Defects located on the specimen's free surface and close to the specimen's free surface were in the case of the rotating bending loading the initiating places for the fatigue cracks what is in agreement with [13, 14, 15, 18, 19].

The defects on the surface act like stress concentrators and the defects in the specimens weaken the specimen cross sections.

The fracture surfaces of examined specimens consist from the fatigue fracture area and the final fracture area, **Fig. 5a**. The fatigue fracture area corresponds to the fatigue crack stable growth. The final fracture region corresponds to the unstable crack growth. In the case of the examined specimens the fatigue fracture region is eccentric due to the position and number of the fatigue crack initiation defects. In all the cases the fatigue cracks were initiated on the specimens' free surfaces and in the fatigue cracks initiation places the casting defects were present, **Fig. 5b - c**.

The defects that caused the fatigue crack initiation were compared with the predicted defect sizes identified by the $area^{1/2}$ and the max. Ferret diameter sizes. The sizes of the defects observed on the fracture surfaces were larger compare to the predicted values, but the relation was retained, i.e. the defects in the initiation places were smaller in the case of the specimens with smaller predicted largest defect sizes and in case of the specimens with the larger predicted defects size the fatigue crack initiating defects were larger. A dependence of the fatigue life to the number of the fatigue crack initiation places was also found [16-20].

DOI 10.12776/ams.v19i3.164 p-ISSN 1335-1532
e-ISSN 1338-1156

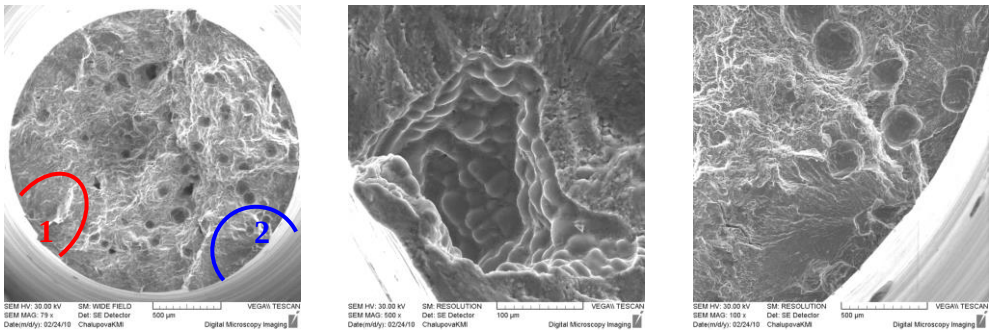

a) fatigue fracture surface with two initiation places

b) defect in the fatigue crack initiation place 1

c) defect in the fatigue crack initiation place 2

Fig. 5 Specimen 7C (cast after the modification by Sr and gassing by the Begaser tablets), S_a = 35 MPa, N_f = 380 467 cycles to failure, SEM

4 Conclusions

This study was aimed at the evaluation of the influence of the used modifier and the casting process on porosity and fatigue behavior using the casting pore size description of the LEVD theory and a limited number of specimens. The fatigue tests of different batches of cast AlSi7Mg were performed after the metallographic evaluation of the specimens and the detailed study of their porosity. The following conclusions were reached:

- microshrinkages were observed in all of the specimens;
- in the case of the batch 7 the gas pores originated due to the gassing of the liquid metal before casting;
- the fatigue test results correlated to the largest defects sizes predictions, i.e. the fatigue life increased by the predicted largest defects size decreasing for a given stress amplitude;
- the best fatigue performance was for the specimens cast after the subsiding effect of the modification by pure Na (batch 3);
- the specimens cast after the modification by pure Na (batch 2) and cast after the modification by Sr and gassing by the Begaser tablets (batch 3) had comparable fatigue properties;
- the fatigue behavior depends on size, number and position of pores and not on their shape (microshrinkage or gas pore);
- although the amount of the tested specimens was limited, the correlation of pore sizes and the fatigue behaviour was confirmed.

References

[1] Q. G. Wang, P. E. Jones: The Minerals, Metals and Materials Society and ASM International, Vol. 38, 2007, No. 4, p. 615-621

[2] J-Y. Buffière, S. Savellib, P. H. Jouneaua, E. Mairea, R. Fougèresa: Materials Science and Engineering, Vol. 316, 2001, No. 1, p. 115-126

[3] Q. G. Wang, D. Apelian, D. A Lados: Journal of Light Metals. Vol. 1, 2001, Issue 1, p. 73-84

[4] J.Z. Yi, Y.X. Gao, P.D. Lee, T.C. Lindley: Materials Science and Engineering A, Vol. 386, 2004, Issues 1-2, p. 396-407

DOI 10.12776/ams.v19i3.164 p-ISSN 1335-1532
e-ISSN 1338-1156

[5] P. Li, D.M. Maijer, T.C. Lindley, P.D. Lee: Materials Science and Engineering A, Vol. 460, 2007, p. 20-30
[6] H. R. Ammar, A. M. Samuel, F. H. Samuel: International Journal of Fatigue, Vol. 30, 2008, Issue 6, p. 1024-1035
[7] H. R. Ammar, A. M. Samuel, F. H. Samuel: Materials Science Engineering A, Vol. 437, 2008, Issue 1-2, p. 65-75
[8] Y. Murakami: *Metal Fatigue: Effects of Small Defects and Nonmetallic Inclusions*, first ed., Elsevier, Oxford, 2002
[9] Y.X. Gao, J.Z. Yi, P.D. Lee, T.C. Lindley: Acta Materialia, Vol. 52, 2004, No. 19, p. 5435-5449
[10] R. Konečná, S. Fintová, G. Nicoletto: Key Engineering Materials, Vol. 465, 2011, p. 354 - 357
[11] S. Fintová, R. Konečná, G. Nicoletto: Materials Engineering, Vol. 16, 2009, No. 3, p. 24-28
[12] J. P. Anson, J. E. Gruzleski: Materials Characterization, Vol. 43, 1999, Issue 5, p. 319-335
[13] H. R. Ammar, A.M. Samuela, F.H. Samuel: Materials Science and Engineering A, Vol. 473, 2008, Issues 1-2, p. 65-75
[14] M. Avalle, G. Belingardi, M. P. Cavatorta, R. Doglione: International Journal of Fatigue, Vol. 24, 2002, Issue 1, p. 1-9
[15] H. Arami, R. Khalifehzadeh, M. Akbari, F. Khomamizadeh: Materials Science and Engineering A, Vol. 472, 2008, Issues 1-2, p. 107-114
[16] S. Fintová, V. Konstantová, R. Konečná, G. Nicoletto: *Experimental study of porosity and fatigue behavior*, In.: 17th International Metallurgical & Materials Conference, Hradec nad Moravicí, TANGER Ostrava, CD-ROM (no. 54), 2008
[17] R. Konečná, G. Nicoletto, S. Fintová: *Statistical description of largest pore sizes in cast Al-Si alloys*, In.: 25th Danubia-Adria Symposium on Advances in Experimental Mechanics, ČVUT Praha, Powerprint, 2008, p. 123-124
[18] R. Konečná, G. Nicoletto, S. Fintová: Acta Metallurgica Slovaca Conference, Vol. 1, 2010, No. 2, p. 8-15
[19] R. Konečná, G. Nicoletto, S. Fintová: *Factographic characterization of fatigue crack initiation from casting defects in AlSiMg*, In.: Fractography 2009, Košice: Institute of Materials Research of the Slovak Academy of Sciences, CD-Rom, 2009
[20] G. Nicoletto, R. Konečná, S. Fintová: International Journal of Fatigue, Vol. 41, 2012, p. 39-46

Acknowledgements
Authors thank the support of experimental research by national project VEGA 1/0196/12.